Pergamon

Journal of Structural Geology, Vol. 17, No. 2, pp. 201 to 214, 1995

0191-8141/95 $9.50+0.00

0191-8141(94)E0037-Y

Fault patterns in the Cretaceous and Tertiary (end syn-rift, thermal subsidence) succession of the Porcupine Basin, offshore Ireland

T. MCCANN

GeoForschungs Zentrum Potsolam, Aufgabenbereich 3, Telegrafenberg A26, 14473, Germany

P. M. SHANNON

Department of Geology, University College Dublin, Belfield, Dublin 4, Ireland

and

J. G. MOORE

Conoco (U.K.) Ltd, Park House, 116 Park Street, London W1Y 4NN, U.K.

(*Received* 31 *August* 1993; *accepted in revised form* 9 *March* 1994)

Abstract—Fault lengths, distributions and orientations were determined at six post-Jurassic horizons in the Porcupine Basin, offshore Ireland. Three rifting periods occurred in the Porcupine Basin with fault orientations and lengths measured for the second and third of these. Dominant fault directions changed through time, while remaining broadly parallel to the basin margins, particularly in the southern part of the basin and especially for the larger faults. Observed changes in activity suggest that strain was evenly distributed throughout the basin during the periods of extension. Length population curves for the faults throughout the basin show an approximate straight line log–log relationship between cumulative number and fault length, indicating that the fracture length populations are self-similar over a range of scales. The fault patterns reflect the response to the transition from a syn-rift dominant phase of basin evolution to one where the development was primarily influenced by thermal subsidence with subsidiary rifting.

INTRODUCTION

The Porcupine Basin lies to the west of Ireland and is among the largest of the Irish offshore sedimentary basins (Fig. 1). It is a tongue-shaped basin lying in water depths ranging from 250 m to more than 1700 m. The basin has a north–south trend, oblique to both Caledonian and Variscan structural trends observed onshore, and interpreted and inferred offshore. It is bounded on three sides by shallow basement platforms composed of Precambrian and Lower Palaeozoic metamorphic rocks (Shannon 1991a). The basin is underlain by thinned continental crust (Makris *et al.* 1988), with thinning more pronounced towards the southern end, where probable Early Cretaceous volcanic and intrusive rocks occur (Tate & Dobson 1988, Tate 1993).

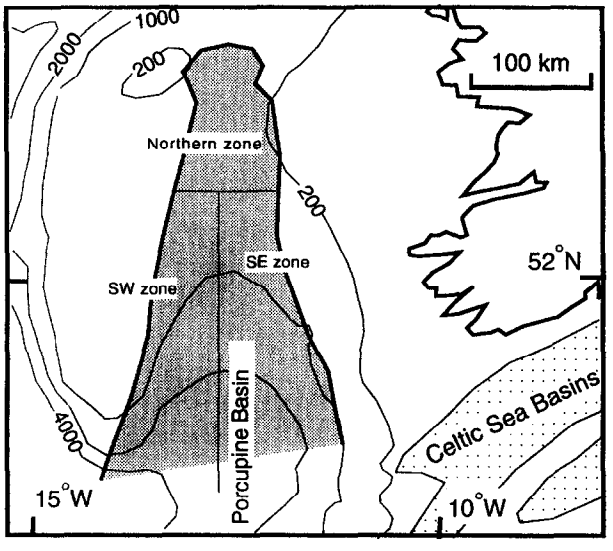

Fig. 1. Map of the Porcupine Basin showing the subdivision into Northern, Southeastern and Southwestern areas.

The Porcupine Basin has a symmetrical profile, with a fault-controlled pre-Cretaceous syn-rift sequence overlain by an extensive succession dominated by the effects of thermal subsidence (Croker & Shannon 1987) giving a general 'steer's head' geometry. The thermal subsidence phase is punctuated by several minor rifting phases. The basin contains up to 13 km of Upper Palaeozoic to Cainozoic sediments.

In this paper we describe the distribution of faults of Cretaceous and Tertiary age with particular reference to their orientations, distributions and lengths. These observations and interpretations are discussed with reference to previous observations of fault orientation in the Porcupine (e.g. Masson & Miles 1986, Max 1986, Masson *et al.* 1987, Makris *et al.* 1988). The objective of this paper is to analyze fault distribution and geometries within the thermal subsidence succession, itself punctuated by several minor rifting phases, at various Cretaceous and Tertiary levels. This should help in understanding the controls on fault location, orien-

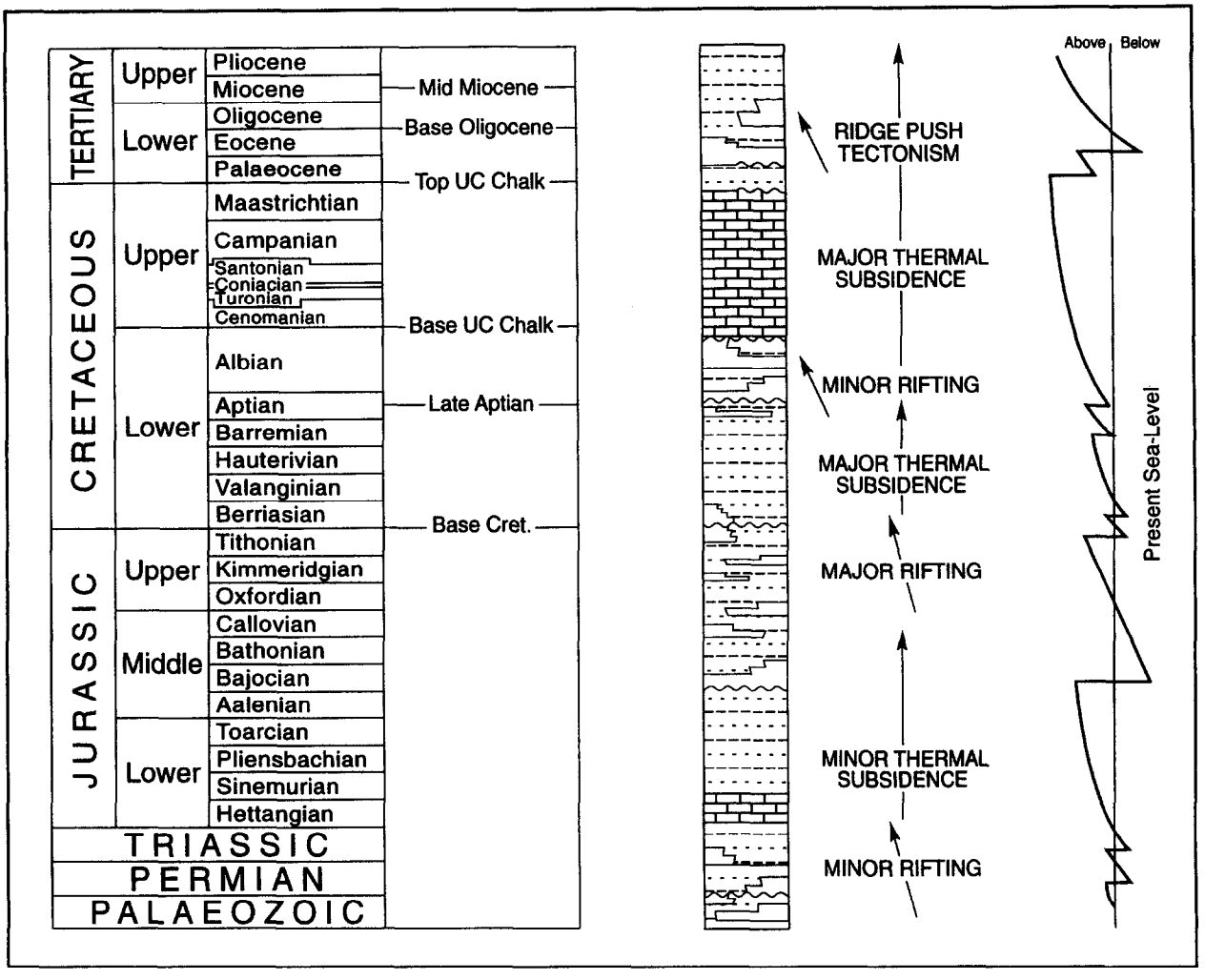

Fig. 2. Stratigraphic column, showing rifting periods, sea-level variations and picked horizons. Based upon Shannon (1991).

tation, distribution and development throughout the basin, as well as assisting with the prediction of fault patterns of different dimensions.

TECTONO-STRATIGRAPHIC SETTING

The crystalline basement of the Porcupine Basin comprises probable Precambrian metasediments and Caledonian granodiorites, leucogranites, quartz syenites, epizonal schists, granulites and charnockites (Roberts *et al.* 1981). The pre-rift succession commences with probable Devonian clastics (Fig. 2) overlain by Dinantian carbonates and clastics (Croker & Shannon 1987, Robeson *et al.* 1988). The Upper Carboniferous, predominantly Westphalian to Stephanian in age, is represented by a deltaic to shallow-marine succession of sandstones, shales and coals. In the northern part of the region, Upper Carboniferous strata are unconformably overlain by continental and marine sediments of Permo-Triassic and Lower Jurassic age, respectively.

In Middle Jurassic times, a change from NE–SW to E–W extension produced a reorganization of structural trends (Shannon 1991b). This extension direction is based on the observation that the predominant normal faults in the region strike broadly N–S. No evidence of any Jurassic strike-slip or significant oblique slip motion on these faults is seen and it is thought likely therefore that the faults are broadly orthogonal to the extension direction. Small northeast–southwest Caledonide-oriented rifts, developed during the Permo-Triassic to Early Jurassic, became redundant and the basin took on its present north–south alignment. Middle Jurassic strata are widespread throughout the basin and typically rest unconformably upon the Upper Carboniferous succession. Middle Jurassic strata are interpreted as continental, comprising braided river and alluvial fan successions giving way to lower energy Upper Jurassic meandering river deposits interdigitated with lacustrine and swamp sediments. These are overlain by marine sediments deposited during a northward-progressing transgression (Croker & Shannon 1987).

Renewed rifting during the Tithonian caused the development of shallow-marine fans and scarp deposits close to the basin margins and adjacent to intrabasinal horsts. The centre of the basin was an area of deep water with the deposition of sand-rich mass flow deposits interdigitating with background hemipelagic sedimentation. Cretaceous strata unconformably overlie the faulted Jurassic succession and represent the rapid tran-

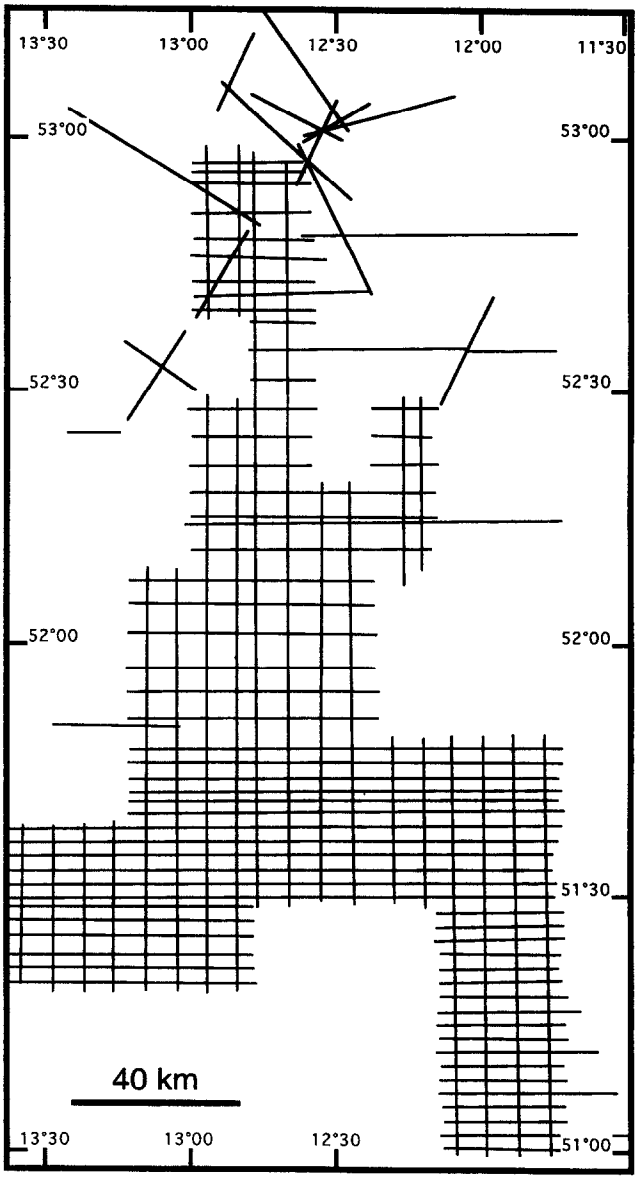

Fig. 3. Map of Porcupine Basin showing the location of the seismic profiles used.

sition (Moore 1992) to the major thermal subsidence stage of basin development. The succession initially comprised deep-water sediments which were overlain by pro-deltaic shales. Locally developed sand-rich deltas with associated beach complexes developed in the Aptian and Albian, reflecting a minor rift phase, and were overlain by the chalk deposited during the Upper Cretaceous marine transgression.

The Tertiary succession comprises pro-deltaic shales overlain by Palaeocene and Eocene sandy delta lobes in the north of the basin (Croker & Shannon 1987). Coeval shales and sandstones further south in the basin are interpreted as submarine fan turbidites and contourites (Shannon 1991a, 1992). An end-Eocene–Oligocene unconformity is followed by deposition of a thick succession of deep-water shales with occasional channelized sandstones which reflect the outpacing of sediment supply by basin subsidence, thereby resulting in a pronounced bathymetric trough.

Water-loaded subsidence curves, based on well-log and seismic data, were used by White *et al.* (1992) to examine subsidence variations within the Porcupine Basin over a period of *c.* 200 Ma. While the results show differences between wells, overall they indicate two periods of rapid increase in subsidence; an early one during the Jurassic (White *et al.* 1992, fig. 2) with a second increase during the early Tertiary (Palaeocene–Eocene). The differences between wells, together with the fact that the wells lie in the northern part of the basin, make it difficult to extrapolate the well results to the entire basin with any degree of confidence.

The first of the three main Porcupine Basin rift phases was initiated as a response to the break-up of Pangaea, and began in the late Triassic. Croker & Shannon (1987) and Conroy & Brock (1989) suggest that early rift directions were controlled by reactivated basement or Caledonian structures, with the N–S trend becoming established in the Middle Jurassic. Makris *et al.* (1988), however, suggested that during this initial phase faults trended N/NNE while the N–S trend only became dominant during the second phase of rifting during Late Jurassic/Early Cretaceous times. This position is broadly supported by Masson *et al.* (1987) who suggest the occurrence of two rifting events in the North Atlantic, although Masson & Miles (1986) suggest that the later rifting event produced NW–SE trending faults. These authors note that this latter trend is the less prevalent of two normal fault trends within the Porcupine Basin. The more dominant trend comprises N–S to NE–SW faults and coincides with the trend of Permian–Triassic to Jurassic basins developed on the continental shelf to the west of Ireland and Britain. This N–S to NE–SW trend in the Porcupine Basin would, therefore, appear to be an older, early Mesozoic trend reactivated during the early Cretaceous rifting episode. A third, minor, rifting phase is suggested by Shannon (1991b) and Shannon *et al.* (1993) to have occurred in Mid Cretaceous times and resulted in local uplift on the basin margins, together with the development of a number of large fan deltas.

The Late Cimmerian unconformity follows a period of pronounced tectonic activity in western Europe and precedes the onset of seafloor spreading north from the Azores (Ziegler 1982). The relative motion of the Western European crustal blocks resulted from the increasing rate of separation of Africa from North America (Naylor & Anstey 1987).

STRUCTURAL CONTROL ON BASIN DEVELOPMENT

The extrapolation of major onshore structures and lineaments to the Porcupine Basin is problematic at best. The Palaeozoic areas of north and northwest Ireland exhibit a clear NE–SW Caledonian trend (Naylor & Anstey 1987). This trend, however, is not reported from the Porcupine Basin and it appears that while there was no obvious deep-seated structural control on basin development (Shannon 1991), small-scale Caledonian trends do occur within the basement. These probably reflect reactivation of a pre-existing Caledonian fabric

Table 1. Fault analysis statistics for the Porcupine Basin. Key: *n*—total numbers; *R*-magnitude—magnitude of vector mean. Figures in brackets refer to values for fault populations greater than or equal to 3 km

	n	Vector mean	Confidence angle	*R*-magnitude
Base Cretaceous SE	42 (30)	347.9 (350.5)	13.99 (11.2)	0.715 (0.857)
Base Cretaceous SW	37 (16)	11.7 (9.9)	10.78 (10.71)	0.844 (0.926)
Base Cretaceous N	51 (20)	13.0 (13.7)	31.77 (50.33)	0.339 (0.344)
Base Cretaceous total	130 (66)	3.0 (359.9)	11.50 (12.42)	0.554 (0.672)
Late Aptian SE	20 (6)	356.9 (5.2)	70.24 (48.98)	0.247 (0.594)
Late Aptian SW	27 (15)	353.3 (0.8)	21.62 (12.54)	0.624 (0.913)
Late Aptian N	48 (31)	15.2 (7.2)	17.76 (14.78)	0.580 (0.759)
Late Aptian total	95 (52)	6.0 (4.9)	15.53 (10.84)	0.488 (0.780)
Base Chalk SE	17 (11)	353.4 (1.6)	76.22 (23.58)	0.247 (0.779)
Base Chalk SW	20 (12)	2.1 (3.0)	55.74 (20.23)	0.311 (0.817)
Base Chalk N	13 (12)	28.2 (25.0)	38.33 (32.57)	0.525 (0.619)
Base Chalk total	50 (35)	10.1 (8.7)	36.56 (16.34)	0.300 (0.691)
Top Chalk SE	70 (51)	1.9 (0.7)	13.21 (6.81)	0.628 (0.910)
Top Chalk SW	46 (27)	356.1 (358.9)	29.78 (16.65)	0.376 (0.736)
Top Chalk N	82 (61)	13.1 (13.5)	12.99 (10.24)	0.602 (0.774)
Top Chalk total	198 (139)	6.0 (5.7)	9.53 (6.3)	0.543 (0.795)
Base Oligocene SE	6 (4)	26.6 (11.1)	50.2 (69.06)	0.581 (0.526)
Base Oligocene SW	4 (3)	351.7 (358.6)	24.37 (9.17)	0.907 (0.994)
Base Oligocene N	46 (41)	358.5 (358.6)	4.73 (5.02)	0.959 (0.955)
Base Oligocene total	56 (48)	359.7 (359.1)	7.23 (6.62)	0.886 (0.918)
Mid Miocene SE	57 (39)	6.5 (3.0)	14.88 (6.83)	0.625 (0.932)
Mid Miocene SW	93 (58)	351.0 (356.9)	27.65 (6.75)	0.293 (0.899)
Mid Miocene N	2 (2)	358.0 (358.8)	11.22 (11.22)	0.998 (0.998)
Mid Miocene total	152 (99)	359.8 (359.4)	14.96 (4.89)	0.411 (0.909)

rather than discrete deep-structural lineaments. The NE–SW Caledonian fault trend noted by MacDonald *et al.* (1987) which controlled the development of the small oil field in Block 26/28 may be related to these.

The existence of offshore equivalents to some of the major onshore lineaments has been suggested (e.g. Bailey 1975, Riddihough & Max 1976, Lefort & Max 1984, Tate 1992). There are, however, a number of problems inherent in attempting to correlate seismic information with onshore mapping, and confusion has resulted. For example, strike-slip faults are interpreted in the basin with dextral offset (Lefort & Max 1984) and sinistral offset (Masson & Miles 1986). The Clare Lineament has been identified as a northwest–southeast magnetic lineament crossing the basin at approximately 51° 30′N (Tate 1992). This feature is associated with a possible change in sedimentation pattern (Naylor & Shannon 1982). The east–west ridge separating the North Porcupine Basin from the Main Porcupine Basin (Naylor & Shannon 1982) was intermittently active from Carboniferous to Early Tertiary times (Croker & Shannon 1987). This structure has been extrapolated by Roberts (1975) to coincide with the Southern Uplands Lineament. Overall, however, there is no compelling evidence to suggest strong control by pre-existing structures on basin development in the Porcupine Basin.

FAULT ORIENTATIONS AND LENGTHS

Fault orientations and lengths were measured for six horizons within the Porcupine Basin. This was based on analysis of approximately 6000 km of multichannel seismic reflection data (Fig. 3). The majority of the data were from the Merlin 1981 regional speculative survey, supplemented by data of various vintages (SA-1975; IP-1976; 77P-1977; PW79-1979; IR80-1980; PR81-1981; P-81-1981; IRL82-1982; BPTIE-1983). All data are of good quality, particularly at Cretaceous and Tertiary levels. Faults were measured throughout the entire basin and were grouped into three constituent areas, namely the Southwestern, Southeastern and Northern zones (Fig. 1). The horizons (with numbers of faults measured per horizon in brackets) analyzed are Late Aptian (95), Base Upper Cretaceous Chalk (50), Top Upper Cretaceous Chalk (198), Base Oligocene (56), and Mid Miocene (152). A further horizon, the Base Cretaceous (i.e. Late Cimmerian, 123) unconformity was analyzed using data published by Naylor & Anstey (1987).

The displacement or throw values along faults were used in determining the strike length of the fault. This was particularly important for those faults which crossed only one seismic line. In certain cases the lengths of these smaller faults could be constrained by the fact that they were small E–W-trending linkage faults between longer N–S-trending basin parallel faults. In other cases their length was determined by the amount of displacement using the relationship between fault length and fault displacement (Watterson 1986, Walsh & Watterson 1988, Walsh *et al.* 1991).

A number of statistical measurements were used in the analysis of the data. These are tabulated in Table 1 and include the Vector Mean, Confidence Angle and R-

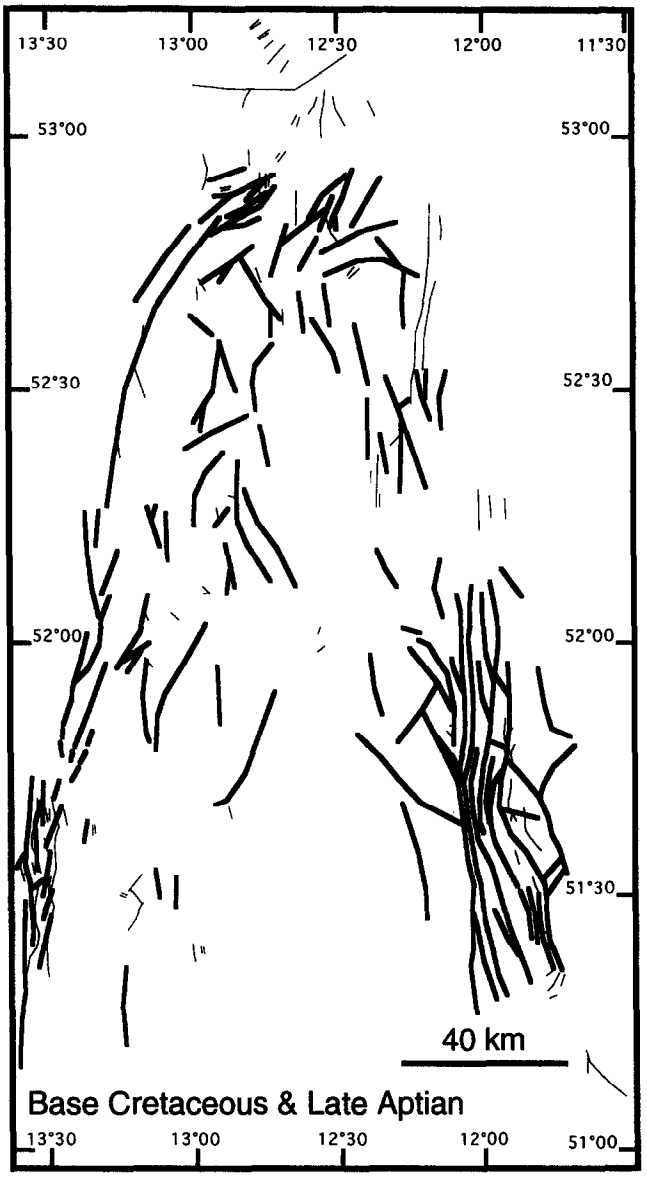

Fig. 4. Fault map of the Base Cretaceous (thick lines) and Late Aptian (thin lines).

Magnitude. Vector Mean is equivalent to strike direction and the Confidence Angle is a measure of the data spread around the Vector Mean. In this case the Confidence Angle has been measured to give a 95% certainty that the true Vector Mean lies within the given limits. R-Magnitude is a measure of data dispersion around the Mean. Large dispersions give a value approaching 0 while those with smaller dispersions will be close to 1.0.

Base Cretaceous (*Figs.* 4 *and* 5)

On a basinwide scale, faults are broadly distributed around the north–south axis with a secondary distribution striking approximately 065°. Within the Southwest zone the predominant direction is NNE–SSW (011.7° vector mean, i.e. average strike) while in the Southeast zone it is dominantly NNW–SSE (347.9° strike). The Northern zone shows a broad distribution of faults, as evidenced by the larger confidence angle (Table 1), without any discernable pattern.

Late Aptian (*Figs.* 4 *and* 6)

A total of 95 faults were mapped from this horizon, just over half of these (48) being in the Northern zone. The orientation is predominantly N–S (006.0° strike). The cumulative number of faults greater than 3 km shows a smaller spread of orientations, with a reduction in confidence angle around the vector mean from 15.53° to 10.84°. This is reflected in the change in the value of the R-magnitude from 0.488 to 0.780, suggesting a smaller dispersion of data points. The numbers of faults recorded in the Southwest and Southeast zones is around half that of the Base Cretaceous, with the Northern zone becoming dominant. Fault orientations remain broadly north–south, with the Northern zone having a greater data spread. There are progressively fewer large faults but these show a pronounced N–S trend (lacking the scatter of the smaller faults) and the Northern zone contains most of the observed faults.

Base Upper Cretaceous Chalk (*Figs.* 7 *and* 8)

Fifty faults are mapped at this horizon and these are concentrated in the Southwest (20) and Southeast (17) zones. The total orientation is broadly NNE–SSW (010.1° strike) with a strong east–west orientation particularly evident in the Southeast zone where the confidence angle is particularly large (Table 1). However, when faults less than 3 km in length are discounted this E–W orientation disappears, since it is a function of shotpoint grid size, and the inability to correlate small faults from line to line, and thereby ascertain their correct orientation. There is a progressively smaller number of large faults but with a pronounced N–S trend (008.7° strike with a confidence angle of 16.34°). The sub-zones show an approximately equal distribution of fault numbers and sizes.

Top Upper Cretaceous Chalk (*Figs.* 7 *and* 9)

A total of 198 faults are mapped at this horizon (the largest number recorded from any horizon) and these are concentrated in the Northern (82) and Southeastern zones (70). The orientation is approximately N–S (006.0° strike) with the greatest number of faults (58) having a north-northeast–south-southwest orientation, reflected in the 9.53° confidence angle. There are progressively fewer large faults, albeit with the dominant north-northeast–south-southwest orientation, the majority of which are in the Northern zone.

Base Oligocene (*Figs.* 10 *and* 11)

Fifty-six faults were mapped at this level throughout the basin, the majority occurring in the Northern zone. Their distribution is broadly N–S (359.7° strike), with some faults trending NE–SW. With increasing fault size the numbers decrease although the N–S trend is preserved. Faults >5 km are present only in the Northern zone.

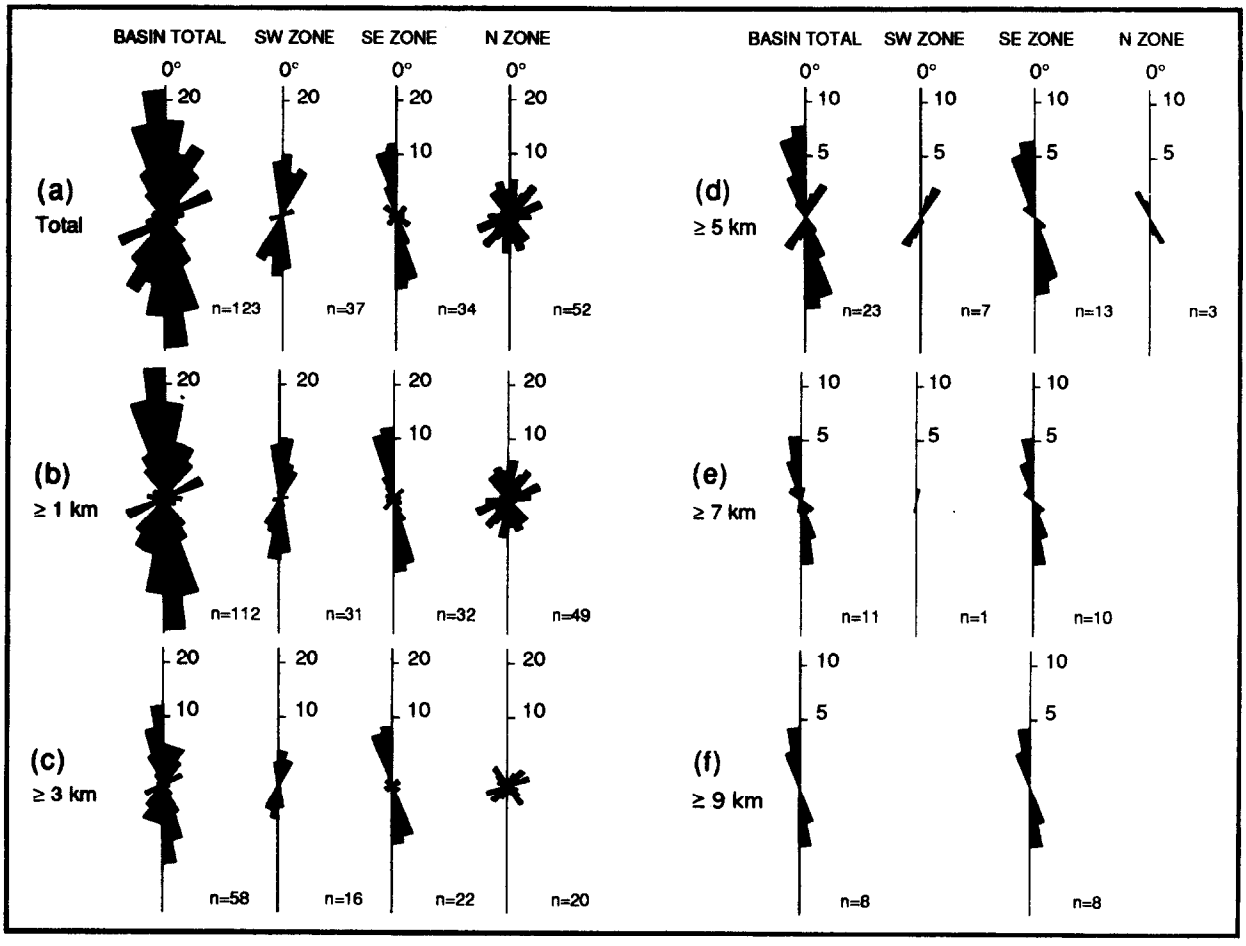

Fig. 5. Rose diagrams showing the distribution of Base Cretaceous age fault orientations within the Porcupine Basin: (a) all faults; (b) faults with lengths greater than or equal to 1 km; (c) 3 km; (d) 5 km; (e) 7 km; and (f) 9 km.

Mid Miocene (*Figs.* 10 *and* 12)

One hundred and fifty-two faults were mapped for this horizon with these being divided almost exclusively into the Southwest and Southeast zones. The predominant orientation is broadly N–S (359.8° strike) with a very strong east–west component, comprising short faults. There is a shift to a more NNE–SSW trend when just larger faults are considered.

DISCUSSION

The main syn-rift stretching phase in the Porcupine Basin occurred at the end of the Jurassic (White *et al.* 1992) and coincided with the end of the major rifting phase, initiated in the Middle Jurassic (Fig. 2). We do not have any data from the earlier Permo-Triassic phase of rifting. Stretching factors (β), for the end Jurassic extension, varied from 1.2 in the north of the Porcupine Basin increasing southwards to greater than 6 (i.e. 30–120 km) (Tate *et al.* 1990, White *et al.* 1992). The fault pattern reflects the response to the transition from a syn-rift dominant phase of basin evolution to one where the development was primarily influenced by thermal subsidence with subsidiary rifting. A Palaeogene extensional phase, suggested by White *et al.* (1992) on the basis of subsidence analysis, with stretching factors of less than 1.1, was coincident with the upper part of the final period of thermal subsidence. However, this is debated by Shannon *et al.* (1993) who argue that the basin subsidence and basin margin uplift are due to ridge-push effects associated with spreading ridge adjustments in the North Atlantic.

Second rifting episode (*Late Jurassic–Early Cretaceous*)

Analysis of the pattern of faulting at the Base Cretaceous shows that faults are oriented parallel to the basin margins in the Southwest and Southeast zones with a more random, albeit broadly north–south, orientation in the Northern zone (Figs. 4 and 5). This is confirmed by the vector means, confidence angles and R-magnitudes for these areas (Table 1). Examination of longer faults indicates that the orientation becomes increasingly aligned to the main trends of the basin margin which are NNE–SSW in the Southwest zone and NNW–SSE in the Southeast zone. Faults in the Northern zone are broadly parallel with, and orthogonal to, the direction of the Southeast zone (particularly for faults >3 km in length). Faults longer than 5 km in the Northern zone trend in the same direction as those in the Southeast zone. Faults are most prevalent in the Southeast zone. According to the stretching model of White *et al.* (1992), faulting should

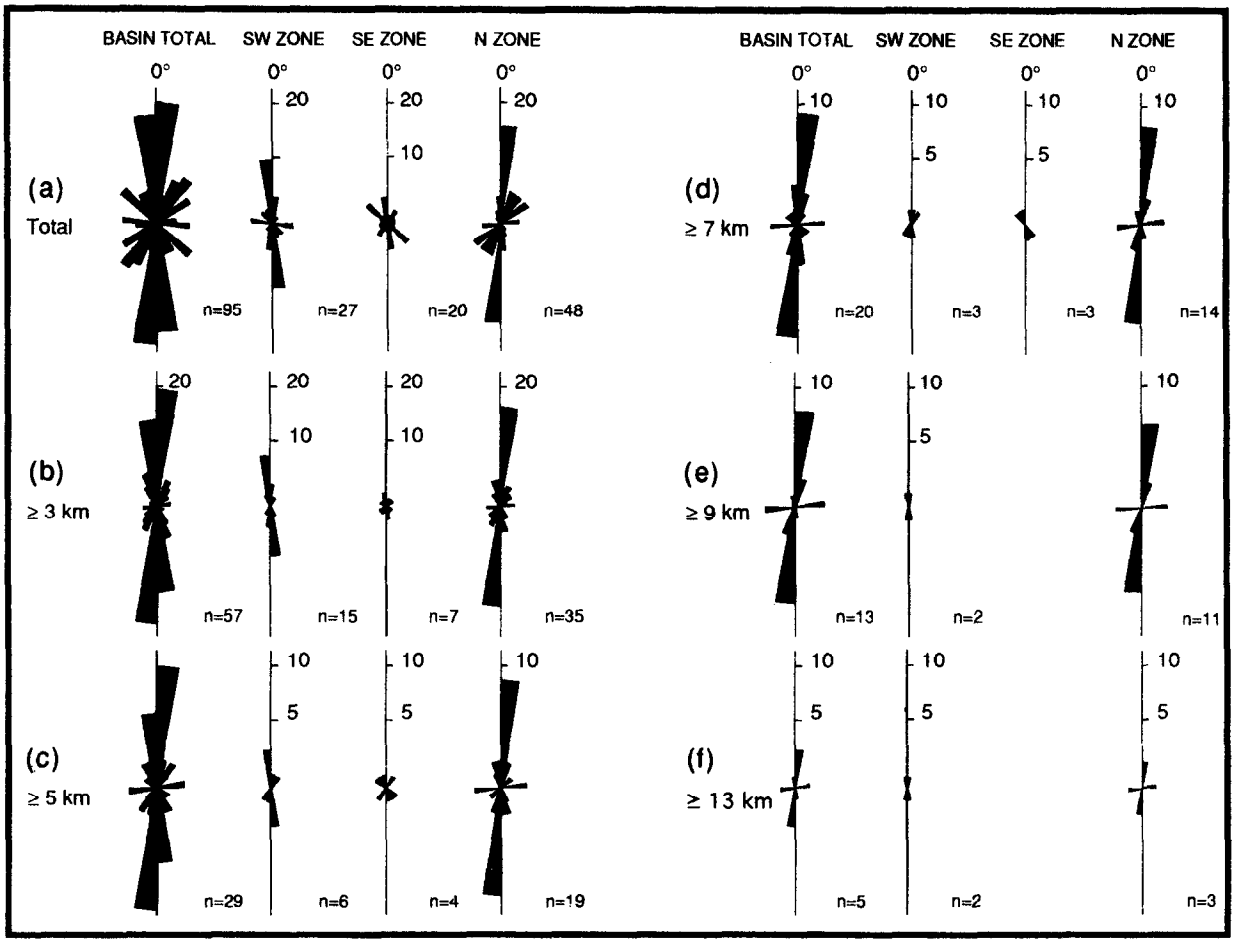

Fig. 6. Rose diagrams showing the distribution of Late Aptian age fault orientations within the Porcupine Basin: (a) all faults; (b) faults with lengths greater than or equal to 3 km; (c) 5 km; (d) 7 km; (e) 9 km; and (f) 13 km.

be seen to increase in the southern parts of the basin, given that the greater amounts of extension occur there. This is broadly the case for the Base Cretaceous horizon where the majority of faults, including larger faults, are recorded from the southern zones. Interestingly, faulting becomes dominant in the Southeast zone once faults less than 3 km are excluded. This concentration might support White *et al.* (1992) in their assertion that the north–south variations in stretching factor were accommodated by a westward clockwise rotation of the Porcupine Ridge away from the Irish shelf by *c.* 25°. Fault orientations in the Northern zone are more variable and with smaller fault dimensions, reflecting a complex basement geology and structural history. It is speculated that this zone could have acted as a pivotal region for the rotation. It should, however, be noted that the faulting recorded at this horizon is merely that of the end of the rifting episode. Given that much of the basin stretching and rotation had occurred prior to the deposition of the earliest Cretaceous sediments, the Base Cretaceous faults may record just the closing phase of the activity. Furthermore, where stretching factors exceed 2, several generations of normal faulting are required to accommodate the extension (e.g. Proffett 1977).

The second rifting episode is widely acknowledged to have had a N–S trend (Makris *et al.* 1988, Masson & Miles 1986, Naylor & Anstey 1987) although a NE–SW trend is also recorded (Masson & Miles 1986). The fault patterns recorded in this study are broadly concurrent with a N–S pattern (003.0° strike) although there is a wide variation within this, as reflected in the R-magnitude (vector mean) value of 0.554 (Table 1). Furthermore, the pattern varies depending on the zone of the Porcupine Basin examined. Indeed the fault pattern for the Northern zone would be difficult to interpret as a north–south one, in anything other than a very broad sense; the R-magnitude value of 0.339 reflects the large dispersion. The NE–SW trend recorded by Masson & Miles (1986), while important, is very much dependent on the zone, and it is only truly apparent for the Southwest zone. Furthermore, as faults increase in length, the north-northwest–south-southeast direction is increasingly dominant. Thus the true situation is more complex and variable than suggested by earlier interpretations.

Third rifting episode (Aptian)

In marked contrast to the Base Cretaceous horizon, the faults of the Late Aptian are concentrated in the Northern zone (50.5%) (Figs. 4 and 6). This horizon was deposited following a period of major thermal subsidence in the Lower Cretaceous and prior to a period of renewed rifting (Fig. 2). The observed fault orientation

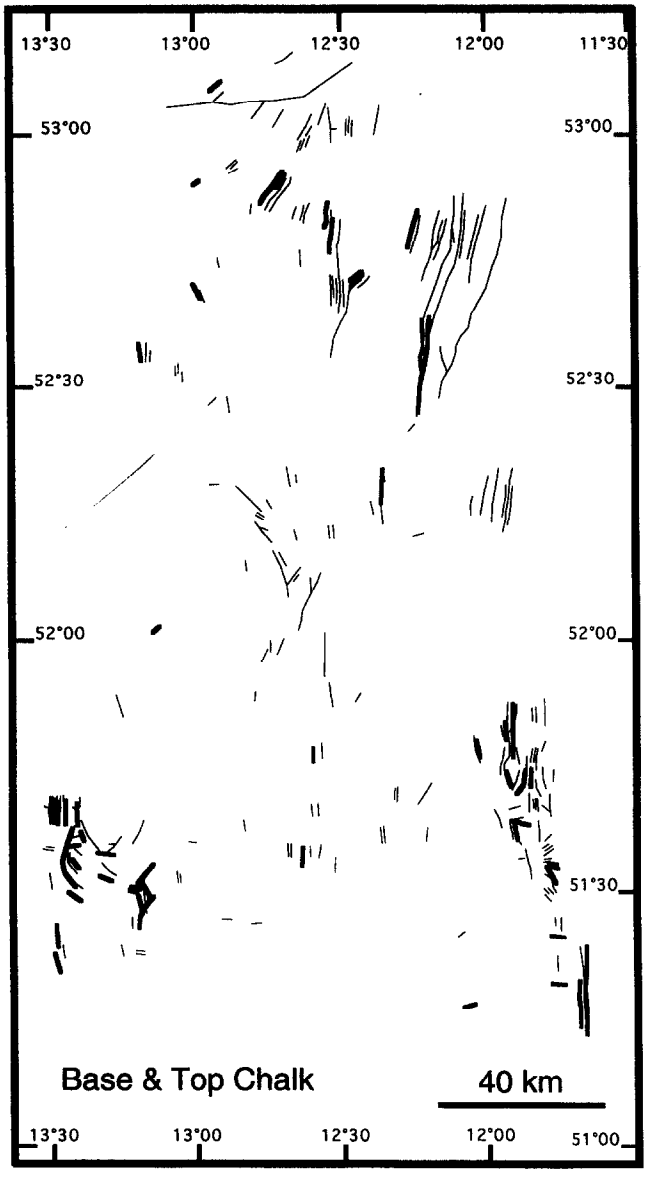

Fig. 7. Fault map of the Base Upper Cretaceous Chalk (thick lines) and Top Chalk (thin lines).

pattern, suggests that brittle deformation and strain at this horizon was almost totally confined to the Northern zone of the basin, although interestingly the orientations measured in this part of the basin are broadly north–south, with less variation than in the underlying horizon. This suggests that the dominant strain direction remained constant with only a shift in locus within the basin. This pattern may be a function of thermal subsidence patterns replicating the dominant underlying fault patterns and being concentrated along those lines. The fact that faulting is concentrated in the Northern zone suggests that subsidence patterns may have been more variable there whereas in the more southerly zones faulting was along the reactivated dominant fault directions. However, if faulting was along reactivated fault directions the faults would be expected to show up on Figs. 7 and 8. Their absence suggests either no extension or the accommodation of extension on small faults below the limit of resolution of our seismic data.

The Base Upper Cretaceous Chalk horizon marks the end of the third, minor rifting phase (Fig. 2). The fault pattern is interesting for a number of reasons. Firstly, the total number of faults is smaller than the two previous horizons (compare Figs. 7 and 4), suggesting a possible decrease in strain, and secondly, the number of faults in the Northern zone is lower than in the two southerly zones (Fig. 8). Indeed, the number of faults remains fairly constant between all three zones for the duration of this third rifting episode, suggesting that strain was evenly distributed throughout the basin during this time.

Final thermal subsidence episode (Late Cretaceous–Late Tertiary)

The largest number of faults recorded in the basin was at the Top Upper Cretaceous Chalk horizon (Figs. 7 and 9) and it is suggested that this is related to lithology. Initially, faults are fairly evenly distributed among the three zones, but the Northern zone is dominant for faults greater than 5 km.

This pattern of fault distribution is again repeated in the Base Oligocene. Here total numbers of faults are greatly reduced, yet they are almost totally concentrated in the Northern zone (Figs. 10 and 11). The lowermost Oligocene sediments were deposited during the proposed Palaeogene stretching phase of White *et al.* (1992). As mentioned earlier the stretching factor suggested by White *et al.* (1992) for this phase, coincident with the upper part of the final period of thermal subsidence, was less than 1.1. The small numbers of recorded faults and their small throws (<50 ms^{-1}), however, would suggest only minor extension. The pattern could, therefore, be interpreted in terms of normal thermal subsidence with superimposed basin margin uplift and accelerated basin centre subsidence cause by ridge-push effects in the Atlantic Ocean.

In contrast, the fault pattern of the Mid-Miocene horizon (with the second largest number of recorded faults) is almost totally dominated by faults in the southerly zones (Figs. 10 and 12). Faulting in the Northern zone is minor with no faults greater than 5 km recorded, although the succession is thin with a maximum thickness of 150 ms^{-1}. Overall the observed pattern shows a possible shift in zones of strain from north to south and back again. Many of these faults are probably related to the syn-sedimentary slumping recorded at this level (see Shannon *et al.* 1993 for location of slumps). The slumping may have been triggered by a relative sea-level fall (Moore & Shannon 1991).

The profile of the Porcupine Basin recorded from the seismic lines and from fault and contour maps (e.g. Naylor & Anstey 1987, figs. 2 and 4) shows that it is essentially a symmetrical basin with a classic 'steer's head' profile. Faults dip towards the basin centre from either margin and at the centre there are relatively unfaulted highs, although this lack of observed faults in the basin centre is probably at least partly due to the lack of seismic resolution. Croker & Klemperer (1989) note

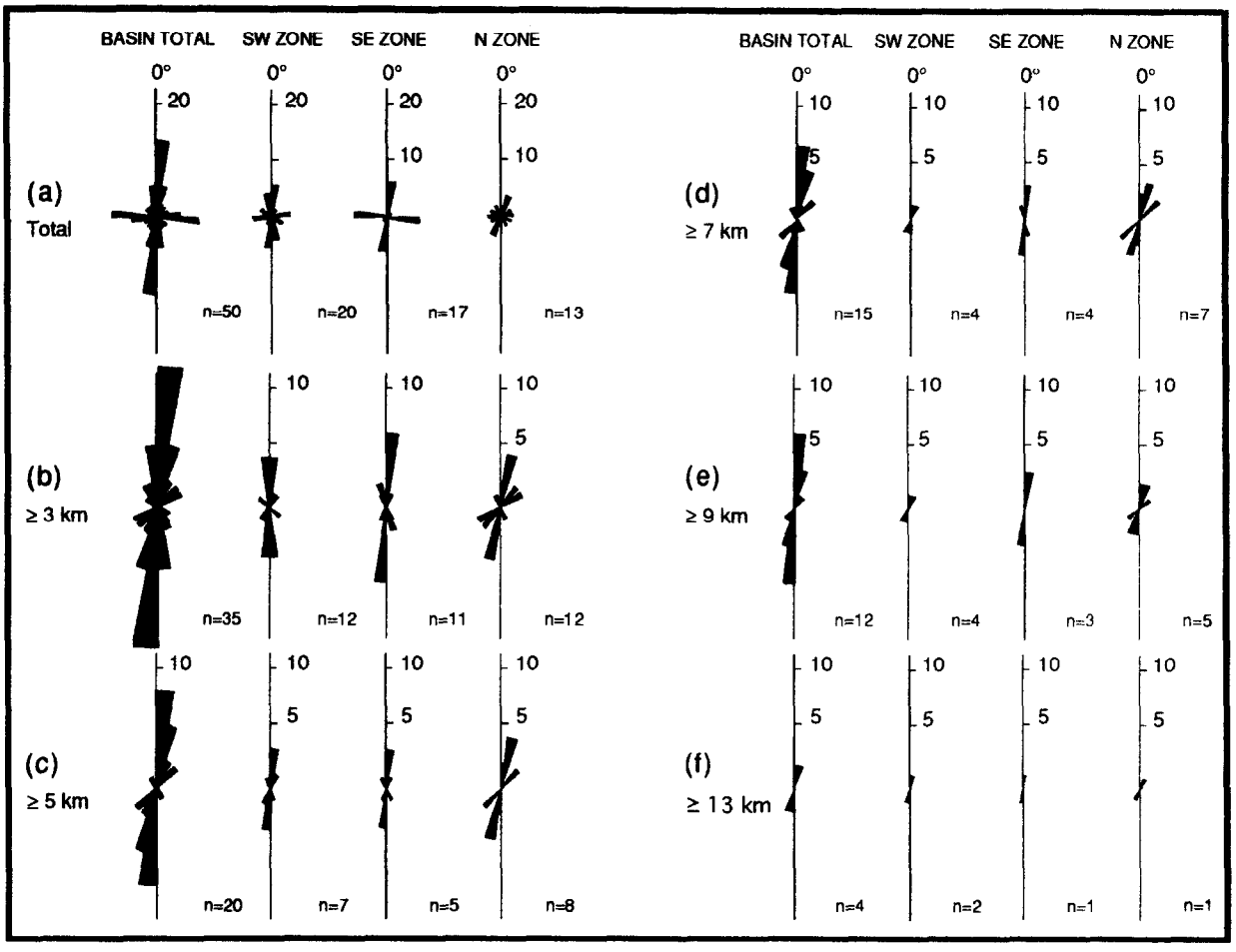

Fig. 8. Rose diagrams showing the distribution of Base Upper Cretaceous Chalk age fault orientations within the Porcupine Basin: (a) all faults; (b) faults with lengths greater than or equal to 3 km; (c) 5 km; (d) 7 km; (e) 9 km; and (f) 13 km.

that the symmetrical profile contrasts with other basins which exhibit asymmetrical systems of multiple half grabens and suggest that the basin was formed by uniform stretching. This inference is supported by initial interpretation of a deep line recorded by the British Institutions' Reflection Profiling Syndicate (BIRPS), which does not show any deep structural control to the basin (Croker & Klemperer 1989). Fault activity does appear to be more dominant on the western edge of the basin (Southwest zone) and this is supported by examination of seismic profiles from that margin. Croker & Klemperer (1989) suggested that the western margin of the basin could be the master fault system for the basin, although this has not yet been confirmed by analysis of deep profiles. It is possible, however, that the stretching as envisaged by White *et al.* (1992), coupled with the rotation of the basin through 25° could have been achieved by greater extension on the western edge of the basin (i.e. Southwest zone). Thus the presence of more and larger faults in the Southeast zone at the Base Cretaceous horizon represents a final adjustment of the basin following the extensional and rotational episode. It is suggested that the faults in the Southwest zone had become work hardened and so the extensional locus switched to the eastern edge.

FAULT SIZE DISTRIBUTION IN THE PORCUPINE BASIN

The size distribution of faults within a fault array can be characterized in terms of either fault length or maximum displacement of faults. The length population curves for the area studied reveal that there is an approximate straight-line relationship, down to the scale of seismic resolution, between the cumulative numbers of faults and the fault length (Fig. 13). The high slopes on the lines are comparable with data from Heffer & Bevan (1990) who suggested that fracture length populations are self-similar over a wide range of scales such that:

$$N = cL^{-2.0} \quad (1)$$

where N is the cumulative number of faults with lengths (L) greater than a given value. This relation is broadly consistent with our fault data. Heffer & Bevan (1990), however, sampled small faults in the Gulf of Suez as a function of horizontal position in two dimensions (2D) from maps. They obtained an exponent -3 for the incremental 2D length-distribution which is consistent with exponent -2 for the cumulative 2D length distribution, or -3 for the cumulative 3D length distribution.

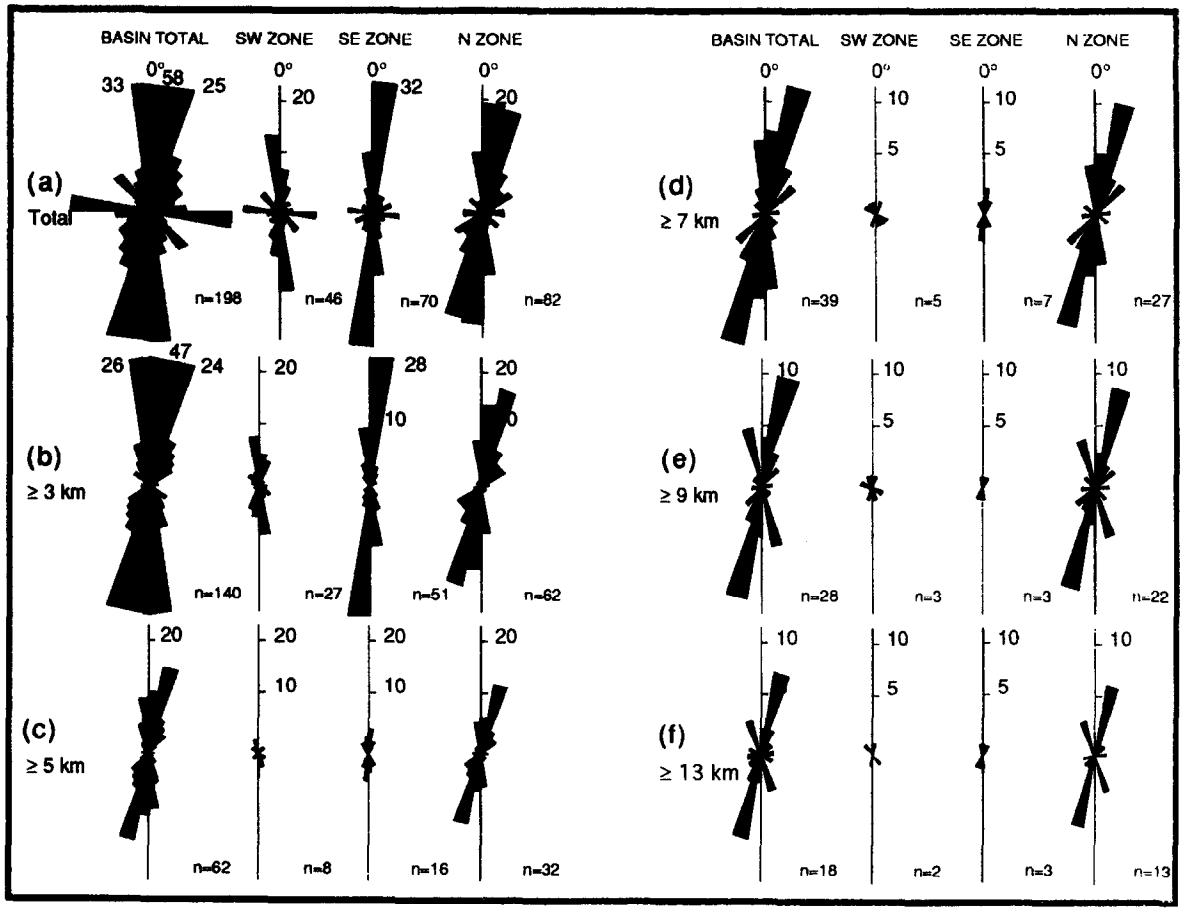

Fig. 9. Rose diagrams showing the distribution of Top Upper Cretaceous Chalk age fault orientations within the Porcupine Basin: (a) all faults; (b) faults with lengths greater than or equal to 3 km; (c) 5 km; (d) 7 km; (e) 9 km; and (f) 13 km.

Several other studies have also obtained exponent −3 for 3D cumulative fault length-distributions and, as shown by Westaway (1992), such distributions are not only expected from the simplest models of fault growth, but are also supported by seismicity (see Westaway 1992 for references).

The slope of *c.* 2.0 for the distribution trends is in accordance with the distributions observed by Scholz & Cowie (1990). Their work was based on samples of mostly large faults (length > brittle layer thickness) and so their distribution does not need correction for the dimensionality of sampling, in that it indicates a 3D distribution of large faults with length exponent −1. It is thus irrelevant that Heffer & Bevan (1992) and Scholz & Cowie (1990) both obtained distributions that can be expressed with exponent −2, because both the types of fault sampled, and the resulting 3D distributions, are different.

In the present study the smallest faults are sampled in one-dimension (1D) along six time horizons that are each treated separately. These faults are too short to cross more than one seismic profile within the seismic grid. The cumulative length-distribution for this sampling method is expected to have exponent −1 if the 3D exponent for small faults is −3. The observed exponent is indeed roughly −1 around length 1–3 km.

For faults with lengths greater than or equal to 3 km each fault is counted only once regardless of how many seismic lines it crosses. This is thus 2D sampling, the two dimensions sampled both being in the horizontal plane. The steeper exponent, roughly −2, of the distribution for lengths 3–10 km is as expected for 2D sampling of a 3D distribution of small faults with length-exponent −3. The flattening of the observed fault distribution below length *c.* 1 km is caused by faults being missed on the seismic profiles, because they have displacements that are too small to be resolved (Fig. 13).

The 1D sample of small faults from the Porcupine Basin has $N_1 \sim 700$ for $L \sim 1$ km. Appropriate theory to quantify strain for such a population of small faults has not yet been published.

Following Westaway (1992), suppose that in 1D sampling of a profile with length W one obtains

$$N_1(D) = a_1 W D^{-c_1} \quad (2)$$

where D is fault displacement. Suppose D is related to L as

$$D = BL^n \quad (3)$$

Typically n is ~1 and B is ~0.01. N_1 can be expressed as a function of L as

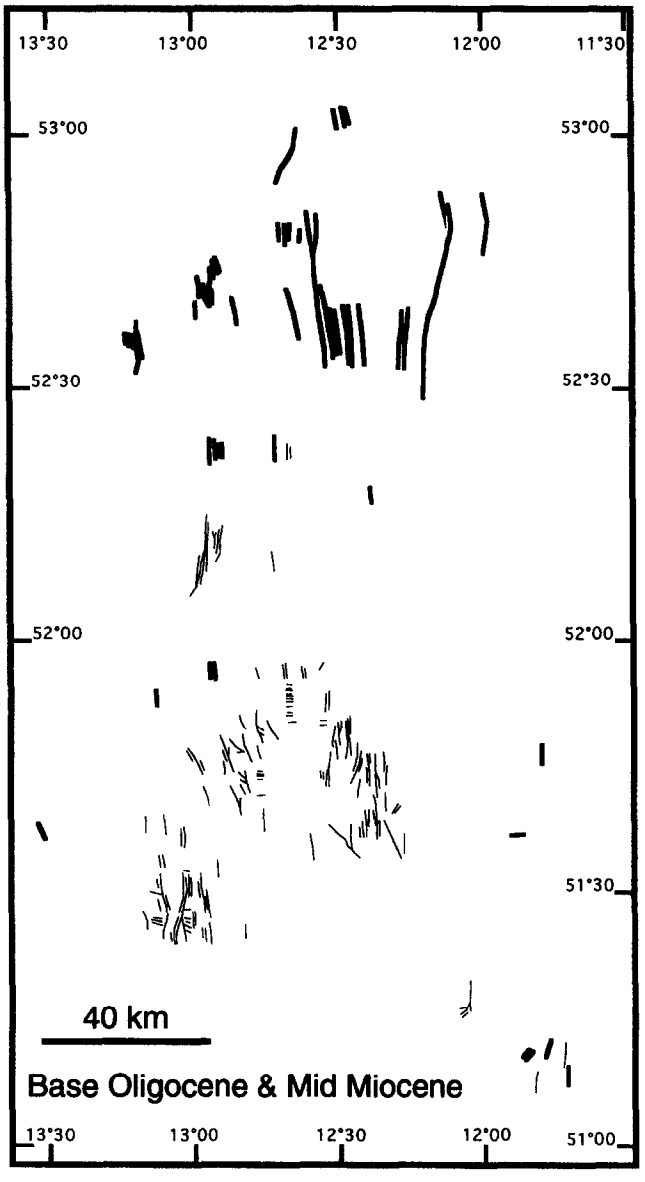

Fig. 10. Fault map of the Base Oligocene (thick lines) and Mid Miocene (thin lines).

$$N_1(L) = a_1 W B^{-c_1} L^{-nc_1}. \quad (4)$$

For the Porcupine Basin, we have 6000 km of seismic profile and 6 1D samples (at $L \cong 1$ km) per profile, so W is 36,000 km. The observed 1D length exponent ($-nc1$) is ~ -1 at $L \cong 1$ km. N_1 is ~700 for $L = 1$ km, so a_1 is c. 2×10^{-4}. The strain contribution ε from small faults with L between L_{min} and L_{max} is

$$\varepsilon = \frac{a_1 n \ln (L_{max}/L_{min})}{2} \quad (5)$$

With $L_{max} \cong 10$ km and $L_{min} \cong 1$ mm, ε is c. 0.0016, which is a very small value.

The 3D number density of faults relates to a_1 as:

$$a = a_1 B^{2/n}(c_1/c). \quad (6)$$

With $B = 0.01$ and $n = 1$, $c_1 = 1$ and $c = 3$, c being the 3D exponent of D, $a_1 = 1.7 \times 10^{-4}$ means that a is $\sim 7 \times 10^{-9}$. It is much less than the limiting value of $\sim 10^{-7}$ that appears appropriate for heavily faulted regions (see Westaway 1992). The bulk of the extensional strain in the Porcupine Basin, therefore, appears to have been associated with large faults with lengths > 10 km, which cut the brittle layer of the crust at the time of extension.

CONCLUSIONS

Fault orientations and lengths in the Porcupine Basin suggest an extensive and complex history related to the interplay of sporadic rift events, basinwide thermal subsidence, North Atlantic seafloor spreading dynamics and syn-sedimentary slumping. Examination of six horizons, three related to rifting and the upper three related to thermal subsidence, suggests that the dominant fault directions changed through time, while remaining broadly parallel to the basin margins. This is particularly true of the Southeast and Southwest zones, while the situation in the Northern zone is more variable. Over time, however, the fault pattern of the Northern zone also becomes more uniform.

Faulting was extensive in the main rift phase (Late Jurassic – Early Cretaceous) with large faults predominant, especially along the east and west basin margins. Fault-orientations were more variable in the Northern zone and are possibly related to the westward clockwise rotation of the Porcupine Ridge away from the Irish Shelf. In the subsequent third rifting episode (Aptian) faults were more localized and concentrated mainly in the Northern zone.

The final thermal subsidence episode (Late Cretaceous–Late Tertiary) also contained the largest number of faults, this being partly a result of lithology. In general, fault distribution patterns during this episode can be interpreted in terms of normal thermal subsidence with superimposed basin margin uplift and accelerated basin centre subsidence related to ridge-push effects in the Atlantic Ocean, and there is no need to invoke a later rifting event. A really restricted faulting in the Tertiary was probably related to Miocene slumping events.

While the fault orientations for a particular horizon may be broadly distributed, as smaller faults are excluded from the analysis then the situation reverts to basin-margin parallelism. Cumulative length population analysis indicates that fracture populations are self similar over a range of scales, and suggests that the bulk of the extension within the Porcupine Basin is associated with large faults (>10 km) which cut the brittle layer at the time of extension.

Acknowledgements—This material is based upon work supported by the EC JOULE project. GECO PRAKLA Exploration Services and the Petroleum Affairs Division of the Irish Department of Energy are thanked for allowing access to well and seismic data. Drs Mark Cooper and Nicky White provided constructive comments on earlier versions of the manuscript, as did Dr Rob Westaway who is further thanked for his input to the final section on fault size distributions.

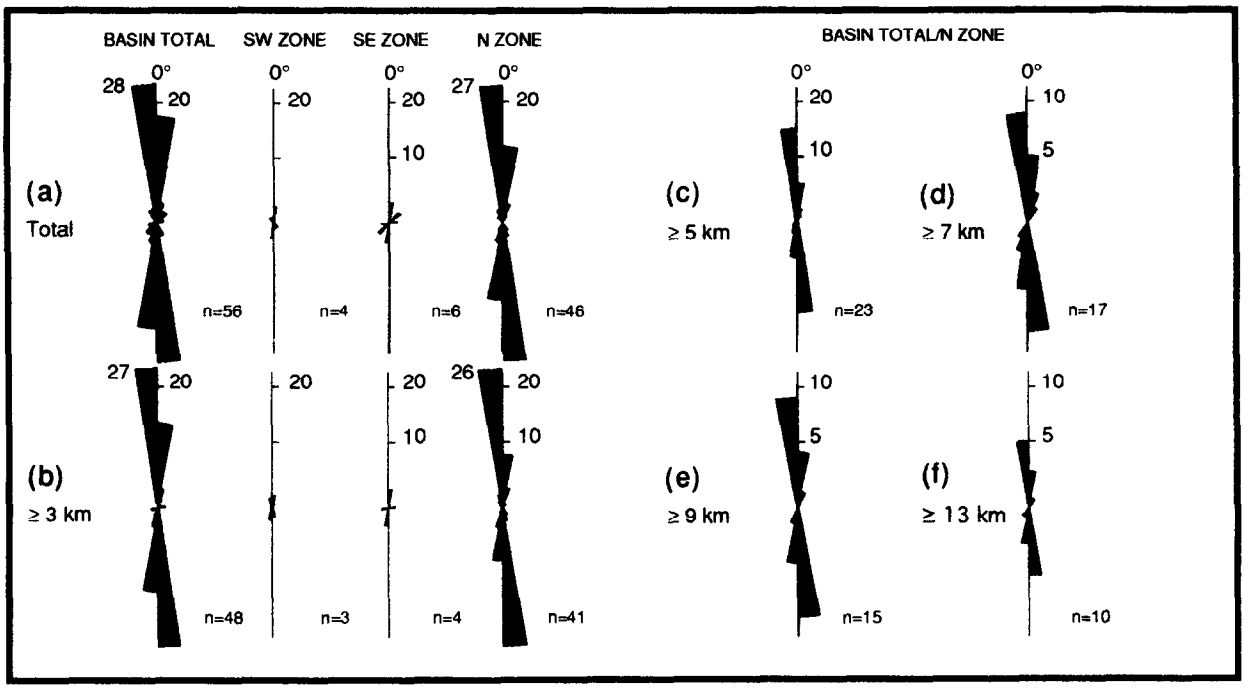

Fig. 11. Rose diagrams showing the distribution of Base Oligocene age fault orientations within the Porcupine Basin: (a) all faults; (b) faults with lengths greater than or equal to 3 km; (c) 5 km; (d) 7 km; (e) 9 km; and (f) 13 km.

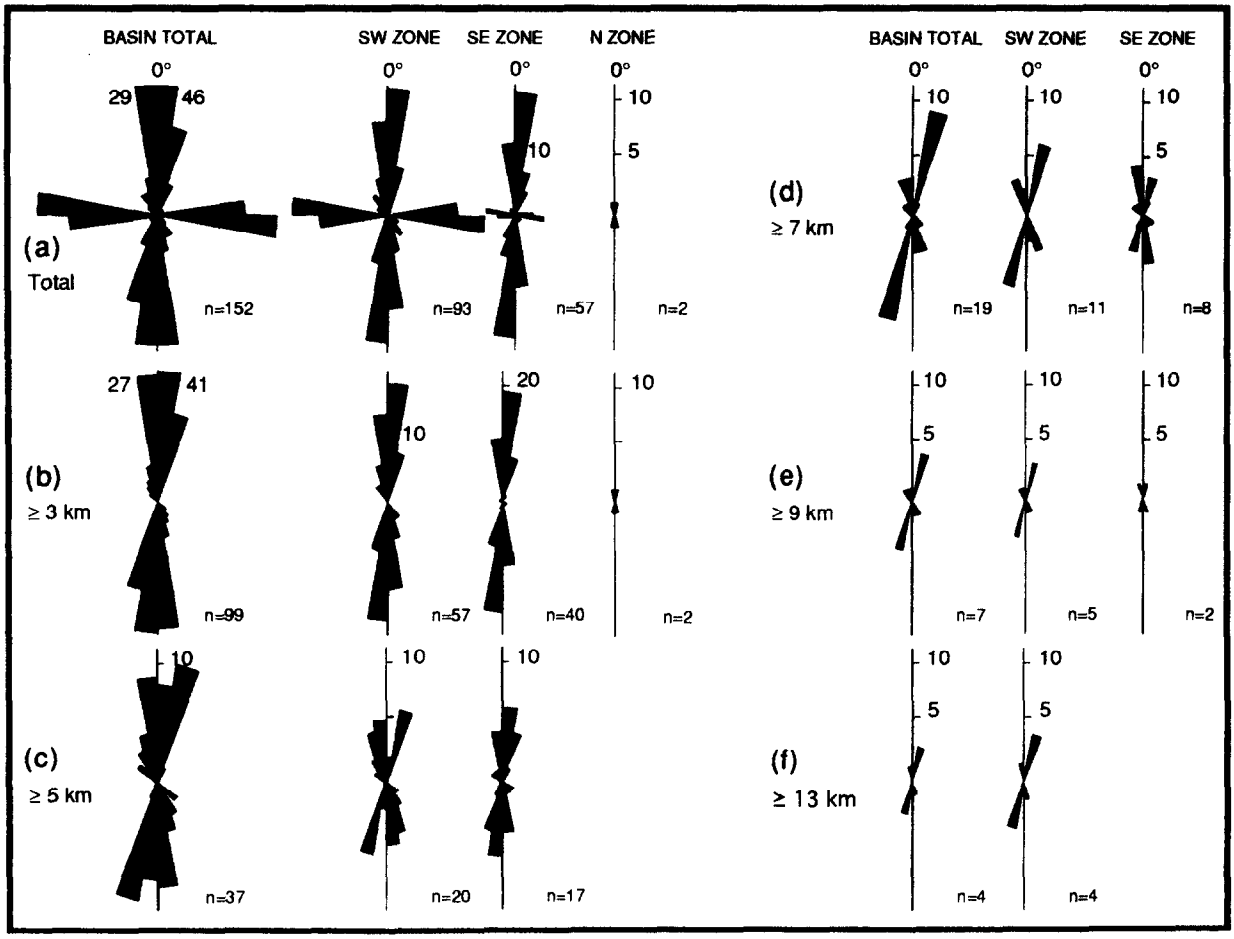

Fig. 12. Rose diagrams showing the distribution of Mid Miocene age fault orientations within the Porcupine Basin: (a) all faults; (b) faults with lengths greater than or equal to 3 km; (c) 5 km; (d) 7 km; (e) 9 km; and (f) 13 km.

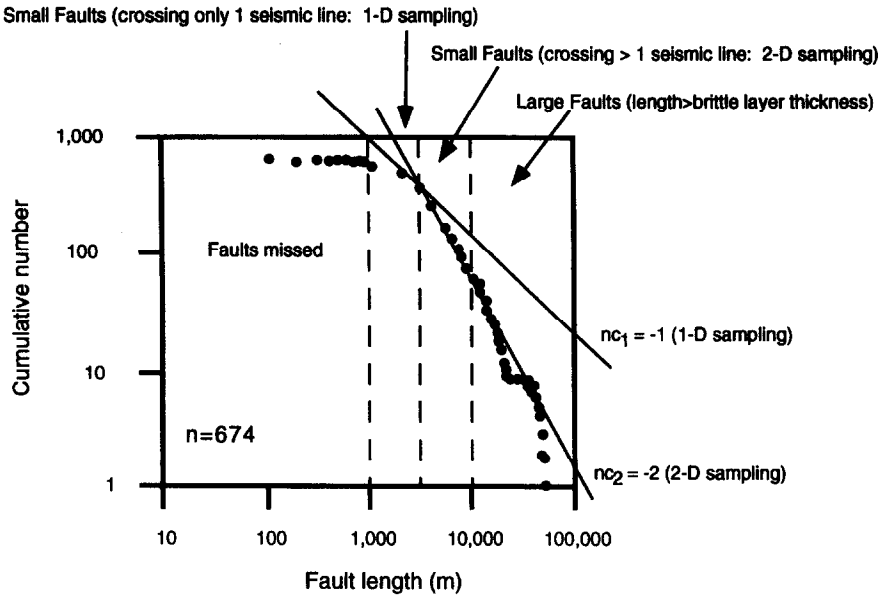

Fig. 13. Cumulative frequency plot of fault lengths in the six measured horizons from the Porcupine Basin.

REFERENCES

Bailey, R. J. 1975. Sub-Cenozoic geology of the British continental margin (Lat. 50°–57°N) and the reassembly of the North Atlantic Late Palaeozoic super-continent. *Geology* **3**, 591–594.

Conroy, J. J. & Brock, A. 1989. Gravity and magnetic studies of crustal structure across the Porcupine Basin west of Ireland. *Earth Plan. Sci. Lett.* **93**, 371–376.

Croker, P. F. & Klemperer, S. L. 1989. Structure and stratigraphy of the Porcupine Basin: relationships to deep crustal structure and the opening of the North Atlantic. In: *Extensional Tectonics and Stratigraphy of the North Atlantic margins* (edited by Tankard, A. J. & Balkwill, H. R.). *Mem. Am. Ass. Petrol. Geol.* **46**, 445–459.

Croker, P. F. & Shannon, P. M. 1987. The evolution and hydrocarbon prospectivity of the Porcupine Basin, offshore Ireland. In: *Petroleum Geology of North West Europe* (edited by Brooks, J. & Glennie, K.). Graham & Trotman Ltd, London, 633–642.

Heffer, K. J. & Bevan, T. G. 1990. Scaling relationships in natural fractures: data, theory and applications. In: *Proc. 2nd European Petrol. Conf.* Society of Petroleum Engineers reprint 20981.

Lefort, J. P. & Max, M. D. 1984. Development of the Porcupine Seabight; the direct relationship between early oceanic and continental structures. *J. Geol. Soc. Lond.* **141**, 663–674.

MacDonald, H., Allan, P. M. & Lovell, J. P. B. 1987. Geology of oil accumulation in Block 26/28, Porcupine Basin, Offshore Ireland. In: *Petroleum Geology of North West Europe* (edited by Brooks, J. & Glennie, K.). Graham & Trotman Ltd, London, 643–651.

Makris, J., Egloff, R., Jacob, A. W. B., Mohr, P., Murphy, T. & Ryan, P. 1988. Continental crust under the southern Porcupine Seabight west of Ireland. *Earth Plan. Sci. Lett.* **89**, 387–397.

Masson, D. G., Dobson, M. R., Auzende, J. M., Cousin, M., Coutelle, A., Rolet, J. & Vaillant, P. 1987. Geology of Porcupine Bank and Goban Spur, Northeastern Atlantic— Preliminary results of the Cyaporc submersible cruise. *Mar. Geol.* **87**, 105–119.

Masson, D. G. & Miles, P. R. 1986. Structure and development of Porcupine Seabight Sedimentary Basin, Offshore Southwest Ireland. *Bull. Am. Ass. Petrol. Geol.* **70**, 536–548.

Max, M. D. 1986. The three-phase development of the Porcupine Seabight: basin formation and the structurally-dependent sedimentary pattern. *J. Petrol. Geol.* **10**, 59–72.

Moore, J. G. 1992. A syn-rift to post-rift transition sequence in the Main Porcupine Basin, offshore western Ireland. In: *Basins on the Atlantic Seaboard: Petroleum Geology, Sedimentology and Basin Evolution* (edited by Parnell, J.). *Spec. Publs Geol. Soc. Lond.* **62**, 333–349.

Moore, J. G. & Shannon, P. M. 1991. Slump structures in the Late Tertiary of the Porcupine Basin, offshore Ireland. *Mar. Petrol. Geol.* **8**, 184–197.

Naylor, D. & Anstey, N. A. 1987. A reflection seismic study of the Porcupine Basin, offshore West Ireland. *J. Earth Sci. Ir.* **8**, 187–210.

Naylor, D. & Shannon, P. M. 1982. *Geology of Offshore Ireland and West Britain*. Graham and Trotman Ltd, London.

Proffett, J. M. Jr. 1977. Cenozoic geology of the Yerington district, Nevada, and implications for the nature and origin of Basin and Range faulting. *Bull. Geol. Soc. Am.* **88**, 247–266.

Riddihough, R. P. & Max, M. D. 1976. A geological framework for the continental margin to the west of Ireland. *J. Geol.* **11**, 109–120.

Roberts, D. G. 1975. Marine geology of the Rockall Plateau and Trough. *Philos. Trans. R. Soc. Lond. Ser. A* **278**, 447–509.

Roberts, D. G., Masson, D. G., Montadert, L. & de Charpal, O. 1981. Continental margin from the Porcupine Seabight to the Armorican Marginal Basin. In: *Petroleum Geology of the Continental Shelf of North-West Europe* (edited by Illing, L. V. & Hobson, G. D.). *Inst. Petrol. Lond.* 455–473.

Robeson, D., Burnett, R. D. & Clayton, G. 1988. The Upper Palaeozoic geology of the Porcupine, Erris and Donegal basins, offshore Ireland. *J. Earth Sci. Ir.* **9**, 153–175.

Scholz, C. H. & Cowie, P. A. 1990. Determination of total strain from faulting using slip measurements. *Nature* **346**, 837–839.

Shannon, P. M. 1991a. Irish offshore basins: geological development and petroleum plays. In: *Generation, Accumulation and Production of Europe's Hydrocarbons* (edited by Spencer, A. M.). *Special Publication of the European Ass. Petrol. Geoscientists* **1**, 99–109.

Shannon, P. M. 1991b. The development of Irish offshore sedimentary basins. *J. Geol. Soc. Lond.* **148**, 181–189.

Shannon, P. M. 1992. Early Tertiary submarine fan deposits in the Porcupine Basin, offshore Ireland. In: *Basins on the Atlantic Seaboard: Petroleum Geology, Sedimentology and Basin Evolution* (edited by Parnell, J.). *Spec. Publs Geol. Soc. Lond.* **62**, 351–373.

Shannon, P. M., Moore, J. G., Jacob, A. W. B. and Makris, J. 1993. Cretaceous and Tertiary basin development west of Ireland. In: *Petroleum Geology of Northwest Europe: Proceedings of the 4th Conference* (edited by Parker, J. R.). The Geological Society, London, 1057–1066.

Tate, M. P. 1992. The Clare Lineament: a relic transform fault west of Ireland. In: *Basins on the Atlantic Seaboard: Petroleum Geology, Sedimentology and Basin Evolution* (edited by Parnell, J.). *Spec. Publs Geol. Soc. Lond.* **62**, 375–384.

Tate, M. P. 1993. Structural framework and tectono-stratigraphic evolution of the Porcupine Seabight Basin, offshore western Ireland. *Mar. Petrol. Geol.* **10**, 95–123.

Tate, M. P. and Dobson, M. R. 1988. Syn- and post-rift igneous activity in the Porcupine Seabight Basin and adjacent continental margin W of Ireland. In: *Early Tertiary Volcanism and the Opening of the NE Atlantic* (edited by Morton, A. C. & Parson, L. M.). *Spec. Publs Geol. Soc. Lond.* **39**, 309–334.

Tate, M. P., White, N. & Conroy, J. J. 1990. Application of the Lithospheric Stretching Model to the Porcupine Seabight Basin, offshore Western Ireland. In: *Post-Devonian Basin Development, North Western Seaboard of the British Isles (Abstracts)*.

Walsh, J. & Watterson, J. 1988. Analysis of the relationship between displacements and dimensions of faults. *J. Struct. Geol.* **10**, 239–247.

Walsh, J., Watterson, J. & Yielding, G. 1991. The importance of small-scale faulting in regional extension. *Nature* **351**, 391–393.

Watterson, J. 1986. Fault dimensions, displacements and growth. *Pure & Appl. Geophys.* **124**, 365–373.

Westaway, R. 1992. Evidence for anomalous earthquake size distributions in regions of minimal strain. *Geophys. Res. Lett.* **19**, 1499–1502.

White, N., Tate, M. & Conroy, J.-J. 1992. Lithospheric stretching in the Porcupine Basin, west of Ireland. In: *Basins on the Atlantic Seaboard: Petroleum Geology, Sedimentology and Basin Evolution* (edited by Parnell, J). *Spec. Publs Geol. Soc. Lond.* **62**, 327–349.

Ziegler, P. A. 1982. *Geological Atlas of Western and Central Europe*. Elsevier, Amsterdam.